Bulletin of Earth Sciences of Thailand

Petrography and mineral chemistry of Cenozoic volcanic rocks in Lop Buri area, central Thailand: Implications for crystallization condition and petrogenesis

Thirawat Tukpho[1], Montree Sirimongkonpun[1] and Alongkot Fanka[2,*]

[1]Department of Geology, Faculty of Science, Chulalongkorn University, Bangkok 10330, Thailand
[2]Applied Mineral and Petrology Special Task Force for Activating Research (AMP STAR), Department of Geology, Faculty of Science, Chulalongkorn University, Bangkok 10330, Thailand
*Corresponding author e-mail: alongkot.f@chula.ac.th

Received: 24 May 2023
Revised: 11 Jul 2023
Accepted: 15 Jul 2023

Abstract

The Cenozoic volcanic rocks distributed in the Lop Buri area, central Thailand, were investigated for petrographic and mineral chemistry studies. The petrographic examination revealed three main rocks: basalt, basaltic tuff, and rhyolite, distinguished by their mineral compositions and textures. Basalt exhibits a trachytic texture, while basaltic tuff is characterized by the presence of pyroclastic materials, including crystal ashes. Rhyolite typically displays a rhyolitic flow and spherulitic texture. Despite the textural differences, basalt and basaltic tuff share similar mineral compositions, predominantly consisting of plagioclase, clinopyroxene, olivine, and accessory opaque minerals of titanomagnetite and titanohematite. In contrast, rhyolite is composed of quartz, K-feldspar, plagioclase, biotite, and titanomagnetite. Further analysis of the magnetite in these volcanic rocks confirmed its primary igneous origin. Crystallization temperature calculations calculated by the magnetite composition indicate temperatures of approximately 758 – 981 °C for basalt, 559 – 738 °C for basaltic tuff, and 672 – 880 °C for rhyolite. These volcanic rocks should be originated from the extensional setting resulted from India-Eurasia collision.

Keywords: Petrography, Geothermometry, Volcanic rock, Loei Fold Belt, Thailand

1. Introduction

Volcanic rocks widely distributed in Thailand and SE Asia are characterized by the presence of various volcanic rock formations from different volcanic events. Although the Palaeozoic to Mesozoic volcanic rocks, including Chiang Mai-Chiang Rai volcanic belt, Tak-Chiang Khong Volcanic belt, Nan-Uttaradit volcanic belt, and Loei-Phetchabun-Ko Chang volcanic belt, have been reported as the most abundant volcanism areas, the Cenozoic volcanic rocks are extensively distributed throughout Thailand and SE Asia (Barr and Cooper, 2013; Barr and Charusiri, 2011; Barr and Macdonald, 1981; Intasopa et al., 1995; Hunyek et al., 2021) (Fig. 1a).

The Cenozoic volcanic rocks are extensively distributed across multiple countries, spanning China, Vietnam, Laos, and Thailand (Barr and Macdonald, 1981; Yan et al., 2018) (Fig. 1a). In Thailand, these volcanic rocks can be found in northern, central, and eastern Thailand, especially along the western and southern edges of the Khorat Plateau (Barr and Macdonald, 1981; Barr and Charusiri, 2011) (Fig. 1a). The Cenozoic volcanic rocks can be chemically divided into basalt and rhyolite (Intasopa et al., 1995). The Cenozoic basalt is predominantly found, but the occurrence of Cenozoic rhyolite has been reported specifically in the Lop Buri area, where it is associated with basalt reported by Intasopa et al. (1995).

Although there are several reports on the whole-rock geochemistry of Cenozoic volcanic rocks in the Lop Buri area (e.g., Barr and Cooper, 2013; Barr and Macdonald, 1981; Chualaowanich et al., 2008a; Chualaowanich et al., 2008b; Intasopa et al., 1995), the details of petrographic characters together with mineral chemistry of magnetite that benefits for crystallization condition of the rocks have not been done.

Therefore, this research aims to study the petrography and mineral chemistry of the Cenozoic volcanic rocks in the Lop Buri area, central Thailand to imply the crystallization condition and the petrogenesis of the volcanic rocks in this area, and to understand the volcanism during Cenozoic in Thailand and SE Asia.

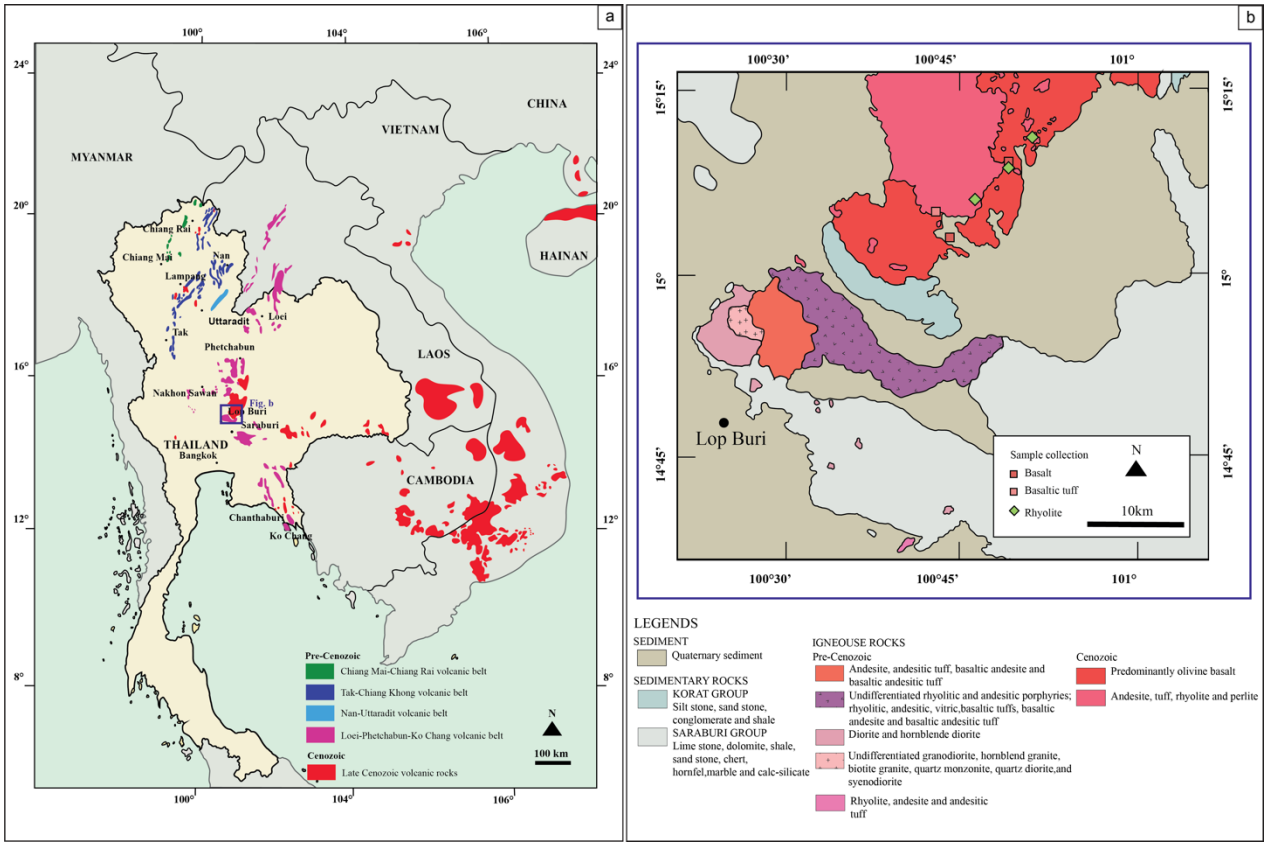

Figure 1 (a) Index map of Thailand and volcanic rocks distribution (modified after Jungyusuk and Khositanont, 1992) (b) Geological map of study area (DMR, 1976)

2. Geological background

Lop Buri Province, central Thailand, the study area (Fig. 1), is composed of diverse rock units, including both sedimentary and igneous rocks. In particular, the sedimentary rocks in the area consist of Permian limestone of Saraburi Group (Assavapatchara et al., 2006), as well as Triassic to Cretaceous clastic sedimentary rocks of Khorat Group (Racey and Goodall, 2009). These sedimentary rocks exhibit a parallel orientation along north-south direction (DMR, 1976; 2007).

The igneous rocks in the study area consist of both volcanic (Intasopa et al., 1995; Uthairat et al., 2021) and plutonic rocks (Nualkhao et al., 2018). Regarding volcanic rocks, Permian-Triassic undifferentiated volcanic rocks and andesitic rocks can be found in the south of the study area while Cenozoic basalt and rhyolite are largely discovered in the middle part of

study area (Fig. 1b). The plutonic rocks are composed of diorite and hornblende diorite (DMR, 1976).

3. Methodology

Sixteen representative samples of volcanic rocks, including basalt, basaltic tuff and rhyolite, were collected from the study area (Fig. 1b). The samples were meticulously prepared as thin sections for petrographic investigation using a polarized light microscope. Following the examination of textures and mineral assemblages, the most suitable and fresh thin sections were carefully selected for further analysis. These selected thin sections were prepared for polished thin sections by polishing process using grinding machines with successively finer abrasives of 6, 3, and 1 microns, respectively.

Subsequently, mineral chemistry study was conducted using an Electron Probe Micro-analyzer (EPMA), specifically the JEOL JXA-8100 model. The analytical conditions were set at 15 kV and approximately 2 μA for a focused beam spot of 1 μm. To ensure accuracy and reliability, mineral and pure oxide standards were utilized for calibration under the same analytical conditions. The calibration process involved automatic ZAF correction, and the results were reported in weight percent oxides. All experiments were performed at Department of Geology, Faculty of Science, Chulalongkorn university.

4. Results

4.1 Field occurrence and petrography

In the study area, a notable association of basalt, basaltic tuff, and rhyolite can be observed. Basalt and basaltic tuff predominantly occur in low-lying areas, such as open-pit mines (Fig 2a), while rhyolitic outcrops are predominantly found as hill and in hilly terrain.

Basalt is generally black, characterized by aphanitic texture, and reddish brown for weathered surface (Fig. 2b). Basaltic tuff is also black like basalt (Fig. 2c). Rhyolitic rocks basically show pale colour for fresh surface and reddish brown for weathered surface. These rhyolitic rocks can be characterized by clear rhyolitic flow texture (Fig. 2d). The detail about collected samples with location are provided in Table 1.

Basaltic rocks are composed of two rock types, including basalt and basaltic tuff. Basalt is characterized by aphanitic and trachytic textures (Fig. 3a), while basaltic tuff is characterized by comprising pyroclastic materials, including ashes and intratelluric crystals (Fig. 3b). However, these rocks show similar mineral assemblages, including predominantly plagioclase showing albite twinning (50 – 60%), clinopyroxene (30 – 40 %), olivine (5 – 10%) and opaque minerals.

Table 1 Representative samples from the study area with sample locations.

Sample No.	Location (Lat/long)	Rock type
B1	15°03'55.9"N /100°57'51.6"E	Basalt
B2	15°03'55.9"N /100°57'51.6"E	Basalt
B3	15°03'55.9"N /100°57'51.6"E	Basalt
B4	15°03'55.9"N /100°57'51.6"E	Basalt
B5	15°03'55.9"N /100°57'51.6"E	Basalt
B6	15°03'55.9"N /100°57'51.6"E	Basalt
B7	15°03'55.9"N /100°57'51.6"E	Basalt
B8	15°03'55.9"N /100°57'51.6"E	Basalt
B9	15°03'55.9"N /100°57'51.6"E	Basalt
B10	15°03'49.2"N /100°57'50.5"E	Basalt
B11	15°12'12.7"N /101°05'27.6"E	Basalt
B12	15°10'07.4"N /101°03'51.0"E	Basalt
B13	15°05'38.3"N /100°57'14.2"E	Basaltic tuff
R1	15°06'41.3"N /100°59'50.1"E	Rhyolite
R2	15°08'19.9"N /101°02'26.3"E	Rhyolite
R3	15°11'27.0"N /101°05'13.9"E	Rhyolite

Rhyolitic rocks in the study area are primarily composed of quartz, K-feldspar (sanidine), plagioclase showing albite twinning, and occasionally biotite. The mineral compositions are approximately quartz (30 – 40%), K-feldspar (20 – 30%), plagioclase (15 – 20%), biotite (5 – 10%) and opaque minerals. In addition, spherulitic texture can be observed in the volcanic rocks (Fig. 3c – 3d).

Opaque minerals can be found as accessory minerals in all volcanic rocks in the study area. these opaque minerals are clearly observed in black colour together with a rectangular shape (Fig. 4a – 4d).

4.2 Mineral chemistry

The mineral chemistry of opaque minerals of the representative polished thin sections of basalt, basaltic tuff, and rhyolite were examined. EPMA data are provided in Table 2. Fe^{2+} and Fe^{3+} concentrations were calculated following Droop (1987).

The mineral chemistry data of the opaque minerals indicate Fe-Ti oxide minerals.

FeO-Fe_2O_3-TiO_2 system of Deer et al. (2013) (Fig. 5) suggested that these Fe-Ti oxide minerals can be deeply classified as follow:

The opaque minerals in basalt are titanomagnetite (TiO_2 ~ 23.4 wt.%, FeO ~ 47.7 wt.%, Fe_2O_3 ~ 40.9 wt.%) and titanohematite (TiO_2 ~ 44.3 wt.%, FeO ~ 35.1 wt.%, Fe_2O_3 ~ 10.3 wt.%).

Figure 2 (a) Outcrop exposure at the open-pit mine of LOMINECHEM CO., LTD at Lop Buri Province and rock samples of (b) basalt showing dark gray to black (c) basaltic tuff showing dark greenish gray (d) rhyolite showing light and yellowish gray to reddish gray layers.

Table 2 Representative EPMA analysis of opaque minerals, including titanohematite and titanomagnetite, in Cenozoic volcanic rocks in the Lop Buri area, central Thailand.

Rock type	Basalt																
Analysis No.	B10_1	B10_2	B10_3	B11_1	B11_2	B11_3	B11_4	B11_5	B11_6	B11_7	B11_8	B11_9	B11_10	B11_11	B11_12	B11_13	B11_14
Sample No.	B10	B10	B10	B11	B11	B11	B11	B11	B11	B11	B11	B11	B11	B11	B11	B11	B11
Mineral	Tianohe-matite	Titanomagnetite															
SiO_2	1.08	0.04	0.09	0.16	0.44	0.10	0.25	0.12	0.07	0.07	0.06	0.19	0.16	0.44	0.10	0.25	0.12
Al_2O_3	0.12	0.50	0.45	1.57	1.09	1.49	1.63	1.31	1.50	1.56	1.39	1.39	1.57	1.09	1.49	1.63	1.31
TiO_2	44.25	7.59	20.98	24.16	23.43	24.80	24.94	24.59	24.43	24.74	23.93	25.04	24.16	23.43	24.80	24.94	24.59
Cr_2O_3	0.06	0.00	0.06	0.01	0.00	0.00	0.00	0.01	0.00	0.01	0.00	0.01	0.01	0.00	0.00	0.00	0.01
FeO_T	44.40	82.99	66.74	62.70	60.35	63.46	61.46	63.89	62.95	63.45	62.65	62.46	62.70	60.35	63.46	61.46	63.89
MnO	2.47	0.20	2.88	0.66	0.62	0.64	0.61	0.75	0.68	0.54	0.65	0.65	0.66	0.62	0.64	0.61	0.75
MgO	1.76	0.91	1.05	3.03	2.50	3.06	3.01	2.69	2.78	2.83	2.86	3.03	3.03	2.50	3.06	3.01	2.69
CaO	0.26	0.05	0.01	0.03	0.19	0.11	0.08	0.15	0.11	0.00	0.00	0.03	0.03	0.19	0.11	0.08	0.15
Na_2O	0.02	0.00	0.00	0.25	0.05	0.10	0.05	0.00	0.05	0.07	0.05	0.14	0.25	0.05	0.10	0.05	0.00
K_2O	0.09	0.02	0.03	0.01	0.04	0.01	0.00	0.00	0.00	0.00	0.01	0.01	0.01	0.04	0.01	0.00	0.00
Total	**94.43**	**92.30**	**92.23**	**92.55**	**88.71**	**93.76**	**92.03**	**93.49**	**92.57**	**93.25**	**91.60**	**92.92**	**92.55**	**88.71**	**93.76**	**92.03**	**93.49**
Si	0.029	0.002	0.004	0.007	0.019	0.004	0.010	0.005	0.003	0.003	0.002	0.008	0.007	0.019	0.004	0.010	0.005
Al	0.004	0.028	0.023	0.076	0.055	0.071	0.079	0.063	0.073	0.075	0.069	0.067	0.076	0.055	0.071	0.079	0.063
Ti	0.898	0.274	0.683	0.748	0.757	0.757	0.770	0.756	0.757	0.760	0.751	0.769	0.748	0.757	0.757	0.770	0.756
Cr	0.001	0.000	0.002	0.000	0.000	0.000	0.000	0.000	0.000	0.000	0.000	0.000	0.000	0.000	0.000	0.000	0.000
Fe	1.002	3.330	2.415	2.158	2.170	2.155	2.110	2.186	2.170	2.168	2.187	2.133	2.158	2.170	2.155	2.110	2.186
Mn	0.056	0.008	0.106	0.023	0.023	0.022	0.021	0.026	0.024	0.019	0.023	0.022	0.023	0.023	0.022	0.021	0.026
Mg	0.071	0.065	0.068	0.186	0.160	0.185	0.184	0.164	0.171	0.172	0.178	0.184	0.186	0.160	0.185	0.184	0.164
Ca	0.007	0.003	0.001	0.001	0.009	0.005	0.004	0.007	0.005	0.000	0.000	0.001	0.001	0.009	0.005	0.004	0.007
Na	0.001	0.000	0.000	0.020	0.004	0.008	0.004	0.000	0.004	0.005	0.004	0.011	0.020	0.004	0.008	0.004	0.000
K	0.003	0.001	0.001	0.000	0.002	0.000	0.000	0.000	0.000	0.000	0.000	0.000	0.000	0.002	0.000	0.000	0.000
Total	**2.073**	**3.711**	**3.302**	**3.218**	**3.199**	**3.207**	**3.182**	**3.207**	**3.206**	**3.202**	**3.214**	**3.196**	**3.218**	**3.199**	**3.207**	**3.182**	**3.207**
Calculated Fe^{2+}, Fe^{3+} following Droop, 1987																	
Fe^{3+}	0.210	1.533	0.731	0.542	0.498	0.516	0.458	0.517	0.514	0.505	0.534	0.490	0.542	0.498	0.516	0.458	0.517
Fe^{2+}	0.792	1.797	1.684	1.616	1.672	1.638	1.652	1.669	1.656	1.663	1.654	1.643	1.616	1.672	1.638	1.652	1.669
TiO_2	44.254	7.585	20.981	24.160	23.426	24.801	24.939	24.586	24.433	24.736	23.928	25.041	24.160	23.426	24.801	24.939	24.586
FeO	35.086	44.791	46.533	46.958	46.497	48.252	48.117	48.782	48.045	48.661	47.366	48.117	46.958	46.497	48.252	48.117	48.782
Fe_2O_3	10.347	42.453	22.456	17.491	15.398	16.895	14.823	16.790	16.564	16.430	16.989	15.938	17.491	15.398	16.895	14.823	16.790
Canil and Lacourse, 2020																	
T (°C)		**758**	**806**	**979**	**952**	**978**	**981**	**955**	**964**	**965**	**969**	**980**	**979**	**952**	**978**	**981**	**955**

Table 2 (Continue)

Rock type	Basalt				Basaltic tuff										Rhyolite		
Analysis No.	B11_15	B11_16	B11_17	B11_18	B13_1	B13_2	B13_3	B13_4	B13_5	B13_6	B13_7	B13_8	B13_9	B13_10	R3_1	R3_2	R3_3
Sample No.	B11	B11	B11	B11	B13	B13	B13	B13	B13	B13	B13	B13	B13	B13	R3	R3	R3
Mineral	Titanomagnetite				Titanohematite			Titanomagnetite									
SiO_2	0.07	0.07	0.06	0.19	0.00	0.00	0.00	0.47	0.98	1.81	0.11	1.29	0.50	0.18	0.25	1.70	0.01
Al_2O_3	1.50	1.31	1.39	1.39	0.05	0.06	0.09	2.16	1.90	1.58	2.04	2.31	1.65	1.64	1.17	2.13	0.50
TiO_2	24.43	24.74	23.93	25.04	47.76	48.12	47.71	13.54	14.28	13.37	12.71	13.16	13.96	14.51	1.88	2.04	1.55
Cr_2O_3	0.00	0.01	0.00	0.01	0.04	0.06	0.03	0.40	0.42	0.14	0.21	0.25	0.23	0.18	0.02	0.00	0.00
FeO_T	62.95	63.45	62.65	62.46	50.45	47.75	47.98	78.74	78.10	78.45	78.49	78.48	78.85	78.30	81.67	80.97	80.07
MnO	0.68	0.54	0.65	0.65				0.95	1.65	1.46	0.77	1.13	0.98	1.64	0.31	0.28	1.10
MgO	2.78	2.83	2.86	3.03	1.10	1.24	1.27	0.73	0.54	0.44	0.68	0.60	0.12	0.28	0.57	0.42	2.11
CaO	0.11	0.00	0.00	0.03	0.00	0.00	0.00	0.00	0.02	0.02	0.00	0.00	0.00	0.00	0.00	0.00	0.00
Na_2O	0.05	0.07	0.05	0.14	0.01	0.03	0.09	0.05	0.02	0.03	0.00	0.07	0.00	0.00	0.04	0.50	0.05
K_2O	0.00	0.00	0.01	0.01	0.01	0.01	0.01	0.03	0.04	0.05	0.01	0.07	0.02	0.00	0.05	0.22	0.00
Total	**92.57**	**93.25**	**91.60**	**92.92**	**99.38**	**97.21**	**97.15**	**96.66**	**97.52**	**97.23**	**94.81**	**97.11**	**96.08**	**96.56**	**85.94**	**88.26**	**85.39**
Si	0.003	0.003	0.002	0.008	0.000	0.000	0.000	0.020	0.041	0.077	0.005	0.055	0.022	0.008	0.013	0.086	0.000
Al	0.073	0.075	0.069	0.067	0.001	0.002	0.003	0.109	0.094	0.079	0.106	0.115	0.084	0.084	0.074	0.126	0.032
Ti	0.757	0.760	0.751	0.769	0.930	0.949	0.944	0.436	0.453	0.426	0.423	0.420	0.456	0.471	0.076	0.077	0.063
Cr	0.000	0.000	0.000	0.000	0.001	0.001	0.001	0.013	0.014	0.005	0.007	0.008	0.008	0.006	0.001	0.000	0.000
Fe	2.170	2.168	2.187	2.133	1.093	1.048	1.055	2.820	2.754	2.783	2.901	2.783	2.862	2.829	3.648	3.409	3.604
Mn	0.024	0.019	0.023	0.022	0.000	0.000	0.000	0.034	0.059	0.053	0.029	0.041	0.036	0.060	0.014	0.012	0.050
Mg	0.171	0.172	0.178	0.184	0.042	0.048	0.050	0.047	0.034	0.028	0.045	0.038	0.008	0.018	0.046	0.032	0.169
Ca	0.005	0.000	0.000	0.001	0.000	0.000	0.000	0.000	0.001	0.001	0.000	0.000	0.000	0.000	0.000	0.000	0.000
Na	0.004	0.005	0.004	0.011	0.001	0.002	0.005	0.004	0.001	0.003	0.000	0.006	0.000	0.000	0.004	0.049	0.006
K	0.000	0.000	0.000	0.000	0.000	0.000	0.000	0.002	0.002	0.003	0.000	0.004	0.001	0.000	0.003	0.014	0.000
Total	**3.206**	**3.202**	**3.214**	**3.196**	**2.069**	**2.050**	**2.057**	**3.486**	**3.453**	**3.457**	**3.516**	**3.469**	**3.477**	**3.476**	**3.877**	**3.805**	**3.924**
Calculated Fe^{2+}, Fe^{3+} following Droop, 1987																	
Fe^{3+}	0.514	0.505	0.534	0.490	0.200	0.147	0.167	1.115	1.050	1.058	1.174	1.081	1.098	1.095	1.810	1.693	1.884
Fe^{2+}	1.656	1.663	1.654	1.643	0.893	0.900	0.889	1.706	1.704	1.725	1.727	1.701	1.765	1.734	1.837	1.716	1.721
TiO_2	24.433	24.736	23.928	25.041	47.762	48.122	47.706	13.544	14.281	13.371	12.713	13.162	13.962	14.513	1.882	2.041	1.551
FeO	48.045	48.661	47.366	48.117	41.229	41.040	40.397	47.619	48.316	48.617	46.719	47.982	48.613	47.987	41.134	40.762	38.226
Fe_2O_3	16.564	16.430	16.989	15.938	10.250	7.454	8.425	34.580	33.103	33.152	35.302	33.891	33.598	33.688	45.045	44.685	46.500
Canil and Lacourse, 2020																	
T (°C)	**964**	**965**	**969**	**980**				**739**	**704**	**681**	**731**	**715**	**560**	**635**	**706**	**673**	**880**

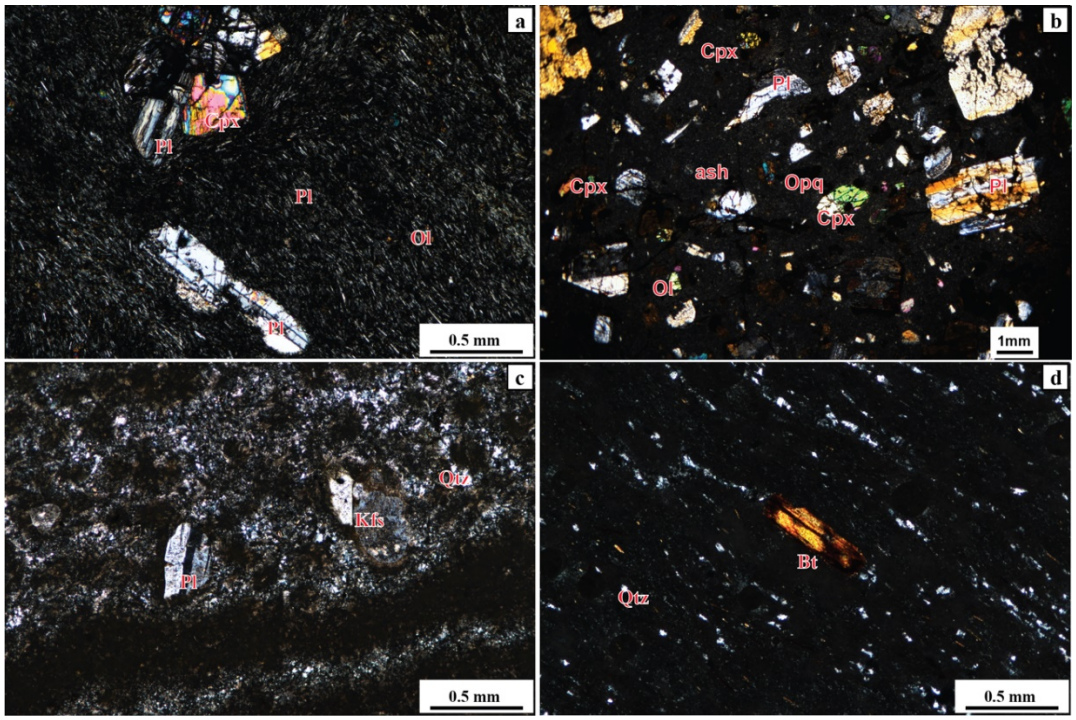

Figure 3 Photomicrographs under cross-polarized light (XPL) showing mineral assemblages and typical textures: (a) Basalt showing trachytic texture, (b) Basaltic tuff (c – d) Rhyolite. Mineral abbreviations: Qtz (quartz); Pl (plagioclase); Kfs (K-feldspar); Cpx (clinopyroxene); Bt (biotite); Opq (opaque minerals) and Ol (olivine) according to Kretz (1983).

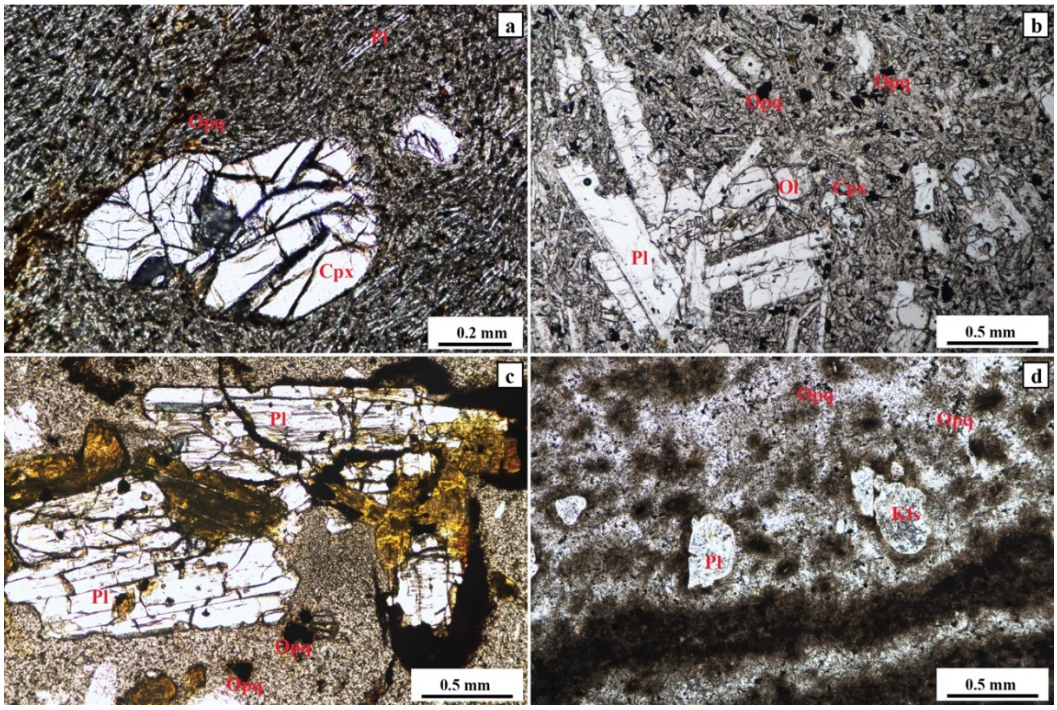

Figure 4 Photomicrographs under plain-polarized light (PPL) showing mineral assemblages and opaque minerals distribution in volcanic rocks: (a – b) Basalt (c) Basaltic tuff (d) Rhyolite. Mineral abbreviations: Qtz (quartz); Pl (plagioclase); Kfs (K-feldspar); Cpx (clinopyroxene); Bt (biotite); Opq (opaque minerals) and Ol (olivine) according to Kretz (1983).

The opaque minerals in basaltic tuff are titanomagnetite (TiO_2 ~ 13.7 wt.%, FeO ~ 48.0 wt.%, Fe_2O_3 ~ 33.9 wt.%) and titanohematite (TiO_2 ~ 47.9 wt.%, FeO ~ 40.9 wt.%, Fe_2O_3 ~ 8.7 wt.%). For the rhyolite, opaque minerals are titanomagnetite (TiO_2 ~ 1.8 wt.%, FeO ~ 40.0 wt.%, Fe_2O_3 ~ 45.4 wt.%).

Titano-magnetite is cubic solid solution at high temperature between magnetite and ulvospinel (Bowles, 2021). Titano-hematite seem to be a result from oxidation of ulvospinel at high temperature following the relationship between magnetite and other Fe-Ti Oxides proposed by Bowles (2021).

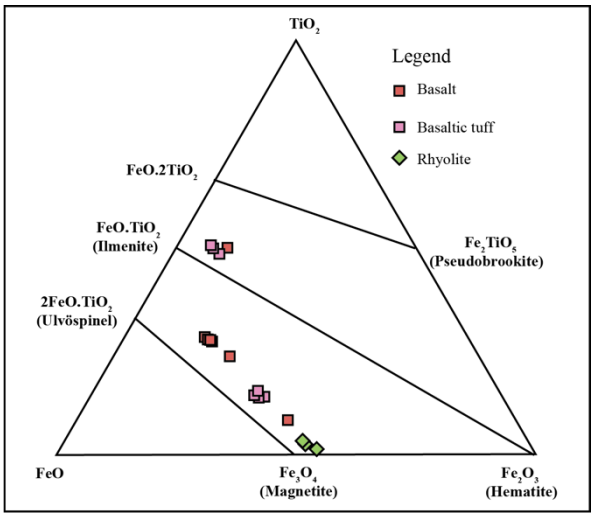

Figure 5 The FeO-Fe_2O_3-TiO_2 system of oxide mineral (Deer et al., 2013).

5. Discussion

5.1 Crystallization condition

The mineral chemistry of a single grain of magnetite can indeed provide valuable information for the calculation of empirical geothermometry according to proposed formula by Canil and Lacourse, (2020), as the following equation:

$$T_{Mg}\ (°C) = -8344 / [\ln X_{Mg} - 4.1] - 273$$

Based on the formula above, the calculated temperature ranges for the crystallization of magnetite in basalt, basaltic tuff, and rhyolite are 758 – 981 °C, 559 – 738 °C, and 672 – 880 °C, respectively.

These magnetite minerals are supposed to be the primary igneous magnetite which can be characterized by crystallization temperature mostly above 700 °C (Canil and Lacourse, 2020). Thus, these calculated temperatures indicate crystallization temperature of magnetite before the eruption of lava generating these rocks to the Earth's surface. The obtained lower temperatures could be attributed to slow cooling processes (Canil and Lacourse, 2020). Therefore, the results imply that the basaltic magmatic system generates at the highest temperature, followed by the rhyolite, and basaltic tuff systems, respectively. This finding is similar to the studies of mafic to more evolved pyroclastic deposits in Popocatépetl volcano, Mexico, which magnetite yields lower crystallization temperature compared to primary mafic to more evolved magmas (Mangler et al., 2020; Dudzisz et al., 2022).

5.2 Petrogenesis and tectonic setting

According to the field occurrence of the Cenozoic volcanic rocks and the petrological characteristics combined with the previous geochemical characters from previous studies (e.g., Barr and James, 1990; Yan et al., 2018), the Cenozoic volcanic rocks in Thailand and Southeast Asia might be originated from extensional setting resulted from India-Eurasia collision (Barr and Charusiri, 2011; Vu et al., 2023).

Based on the conducted petrographic study, it was determined that the Cenozoic volcanic rocks in the study area are predominantly composed of basaltic and rhyolitic rocks. These characteristics of these volcanic rocks are commonly observed in extensional-related settings, such as the volcanism of the High Lava Plains and Northwestern Basin and Range in Oregon (Ford et al., 2013), as well as in locations like

Iceland, characterized by significant basalt and rhyolite formations (Zellmer et al., 2008). The Ethiopian Rift also exhibits volcanic activity featuring basalt and rhyolite compositions (Mohr and Gouin, 1976). In addition, trachytic texture widely found in basalt in the study area, which it indicates basaltic lava flow (Smith, 2002), can be commonly found in extensional setting (Camp et al., 2003; Hooper et al., 2010).

6. Conclusion

The Cenozoic volcanic rocks found in the Lop Buri area comprise basalt, basaltic tuff, and rhyolite. Both basalt and basaltic tuff are primarily composed of plagioclase, clinopyroxene, olivine, and opaque minerals classified as titanohematite and titanomagnetite. The rhyolite, on the other hand, mainly consists of quartz, K-feldspar, plagioclase, biotite, and opaque minerals as titanomagnetite. The titanomagnetite present in all volcanic rocks indicates the primary igneous magnetite. Mineral chemistry analysis of magnetite suggests that the basalt was crystallized at the highest temperature, approximately 758 – 981 °C, compared to basaltic tuff and rhyolite which crystallized at 672 – 880 °C and 559 – 738 °C, respectively. The combination studies well support the suggestion that the Cenozoic volcanic rocks in Thailand and Southeast Asia might be originated from the extensional setting.

Acknowledgements

The authors would like to express their gratitude to MINECHEM company for allowing us to investigate the outcrop and collect rock samples from their mining site. We would also like to extend our appreciation to Miss Sopit Poompuang for her valuable guidance in conducting the EPMA work. Finally, we would like to thank the Department of Geology, Faculty of Science, Chulalongkorn University, for their continuous support. This research was financially supported by Sci-Super VI fund from Faculty of Science, Chulalongkorn University.

References

Assavapatchara, S., Charusiri, P., Charoentitirat, T., Chutakositkanon, V., Hisada, K. & Ueno, K. 2006. On the lithostratigraphy of Permian rocks in Thailand: implications for depositional environments and tectonic settings. *Journal of the Geological Society of Thailand*, 27-48.

Barr, S. & Cooper, M. 2013. Late Cenozoic basalt and gabbro in the subsurface in the Phetchabun Basin, Thailand: Implications for the Southeast Asian Volcanic Province. *Journal of Asian Earth Sciences*, 76, 169-184.

Barr, S. M. & Charusiri, P., 2011. Volcanic Rocks. In M. F. Ridd, A. J. Barber, & M. J. Crow (Eds.), *The Geology of Thailand*, pp. 415-439. London: The Geological Society.

Barr, S.M. & James, D.E. 1990. Trace element characteristics of Upper Cenozoic basaltic rocks of Thailand, Kampuchea and Vietnam. *Journal of Southeast Asian Earth Sciences,* 4, 233-242.

Barr, S.M. & Macdonald, A.S., 1981. Geochemistry and geochronology of late Cenozoic basalts of Southeast Asia: Summary. *GSA Bulletin* 92, 508-512.

Bowles, J.F.W. 2021. Oxides, In: Alderton, D., Elias, S.A. (Eds.), *Encyclopedia of Geology (Second Edition)*. Academic Press: Oxford, 428-441.

Camp, V.E., Ross, M.E. & Hanson, W.E. 2003. Genesis of flood basalts and Basin and Range volcanic rocks from Steens Mountain to the Malheur River Gorge, Oregon. G*eological Society of America Bulletin,* 115, 105-128.

Canil, D. & Lacourse, T. 2020. Geothermometry using minor and trace elements in igneous and hydrothermal magnetite. *Chemical Geology,* 541, 119576.

Chualaowanich, T., Saisuthichai, D. & Sarapanchotewittaya, P., 2008a. *Ar/Ar dating of basalts.* Department of Mineral Resources, Thailand. 67.

Chualaowanich, T., Saisuthichai, D., Sarapanchotewittaya, P., Charusiri, P., Sutthirat, C., Lo, C.H., Lee, T.Y. & Yeh, M.W. 2008b. New Ar/Ar ages of some Cenozoic basalts from the East and Northeast of Thailand. *Proceedings on Interational Symposia on: Geoscience Resources and Envionments of Asian Terranes*. Bangkok, Thailand.

Deer, W.A., Howie, R.A. & Zussman, J., 2013. *An introduction to rock-forming minerals, 3rd ed*. Longman: London, United Kingdom.

DMR. 1976. *Geological map of Thailand, 1st ed.* Geological Survey Division, Department of Mineral Resources, Bangkok, Thailand.

DMR. 2007. *Classification of area for geological and mineral reources management in Lop Buri Province, Bangkok, Thailand*. Department of Mineral Resources, Thailand. 64.

Droop, G.T.R. 1987. A general equation for estimating Fe^{3+} concentrations in ferromagnesian silicates and oxides from microprobe analyses, using stoichiometric criteria. *Mineralogical Magazine,* 51, 431-435.

Dudzisz, K., Kontny, A. & Alva-Valdivia, L.M. 2022. Curie temperatures and emplacement conditions of pyroclastic deposits from Popocatépetl volcano, Mexico. *Geochemistry, Geophysics, Geosystems,* 23, e2022GC010340.

Ford, M.T., Grunder, A.L. & Duncan, R.A. 2013. Bimodal volcanism of the High Lava Plains and Northwestern Basin and Range of Oregon: Distribution and tectonic implications of age-progressive rhyolites. *Geochemistry, Geophysics, Geosystems*, 14, 2836-2857.

Hooper, P., Widdowson, M. & Kelley, S. 2010. Tectonic setting and timing of the final Deccan flood basalt eruptions. *Geology*, 38, 839-842.

Hunyek, V., Sutthirat, C. & Fanka, A. 2020. Magma Genesis and Arc Evolution at the Indochina Terrane Subduction: Petrological and Geochemical Constraints From the Volcanic Rocks in Wang Nam Khiao Area, Nakhon Ratchasima, Thailand. *Frontiers in Earth Science*, 8, p. 271.

Intasopa, S., Dunn, T. & Lambert, R.S. 1995. Geochemistry of Cenozoic basaltic and silicic magmas in the central portion of the Loei–Phetchabun volcanic belt, Lop Buri, Thailand. *Canadian Journal of Earth Sciences,* 32, 393-409.

Jungyusuk, N. & Khositanont, S. 1992. Volcanic rocks and associated mineralization in Thailand. *Proceedings oo National Conference on Geologic Resources of Thailand: Potential for Future, Development*. Amsterdam, Natherland.

Kretz, R. 1983. Symbole for Rock Forming Minerals. *American Mineralogist,* 68, 277–279.

Mangler, M.F., Petrone, C.M., Hill, S., Delgado-Granados, H. & Prytulak, J., 2020. A pyroxenic view on magma hybridization and crystallization at

Popocatépetl volcano, Mexico. *Frontiers in earth Science,* 8, p.362.

Mohr, P. & Gouin, P. 1976. Ethiopian Rift System. *Geodynamics: Progress and prospects,* 5, 81-87.

Nualkhao, P., Takahashi, R., Imai, A. & Charusiri, P. 2018. Petrochemistry of Granitoids Along the Loei Fold Belt, Northeastern Thailand. *Resource Geology,* 68, 395-424.

Racey, A. & Goodall, J.G. 2009. Palynology and stratigraphy of the Mesozoic Khorat Group red bed sequences from Thailand. *Geological Society, London, Special Publications,* 315, 69-83.

Smith, J.V. 2002. Structural analysis of flow-related textures in lavas. *Earth-Science Reviews,* 57, 279-297.

Uthairat, S., Salam, A. & Manaka, T., 2021. Preliminary Petrography and geochemistry of volcanic rocks in Lam Sonthi area, Lop Buri province, central Thailand. *Bulletin of Earth Sciences of Thailand,* 13, 47-58.

Vu, T.A.D., Fanka, A. & Sutthirat, C. 2023. Trace element geochemistry and U-Pb dating of zircon inclusions in sapphire from Southern Vietnam: Indicator of basalt-related sapphire formation. J*ournal of Asian Earth Sciences,* 245, 105537.

Yan, Q., Shi, X., Metcalfe, I., Liu, S., Xu, T., Kornkanitnan, N., Sirichaiseth, T., Yuan, L., Zhang, Y. & Zhang, H. 2018. Hainan mantle plume produced late Cenozoic basaltic rocks in Thailand, Southeast Asia. *Scientific Reports,* 8, p. 2640.

Zellmer, G.F., Rubin, K.H., Grönvold, K. & Jurado-Chichay, Z. 2008. On the recent bimodal magmatic processes and their rates in the Torfajökull–Veidivötn area, Iceland. *Earth and Planetary Science Letters,* 269, 388-398.